THE JOURNAL OF PHYSICAL CHEMISTRY C

Article

Methyl Formate Formation during Methanol Conversion over the (111) Ceria Surface

Ariana Beste, and Steven H. Overbury

J. Phys. Chem. C, **Just Accepted Manuscript** • DOI: 10.1021/acs.jpcc.7b01431 • Publication Date (Web): 19 Apr 2017

Methyl Formate Formation during Methanol Conversion over the (111) Ceria Surface

Ariana Beste*,† and Steven H. Overbury‡

†*Joint Institute for Computational Sciences, The University of Tennessee, Oak Ridge, TN 37831*

‡*Chemical Sciences Division, Oak Ridge National Laboratory, Oak Ridge, TN 37831*

E-mail: bestea@ornl.gov;Phone:865-241-3160

Abstract

We study methyl formate formation during methanol conversion on the fully oxidized and partially reduced ceria (111) surface using density functional theory. Starting from methanol and formaldehyde adsorbed on the surface, we consider two pathways of methyl formate production. Pathway 1 consists of formaldehyde dehydrogenation followed by oxygen-carbon bond formation. Along pathway 2, the oxygen-carbon bond is established prior to intermediate dehydrogenation. Formaldehyde production is observed at elevated temperature at which we expect both pathways to be energetically attainable on the fully oxidized surface. However, the probability of both reactants being adsorbed next to each other is low. This probability can be increased by the reduction of the surface. The partially reduced ceria surface is modelled by the introduction of an oxygen vacancy in the surface. If formaldehyde adsorbs over a vacancy, both pathways potentially contribute to methyl formate formation. In contrast, if methoxide that is obtained by dissociative adsorption of methanol is placed in the vacancy, methyl formate production becomes energetically highly demanding. Still, dehydrogenation of methoxide or methoxide exchange with coadsorbates converts methoxide in a vacancy to an active species for methyl formate formation while increasing the residence time of methoxide on the surface. Importantly, the preference of pathway 1 is due to the promotion of surface bound formaldehyde dehydrogenation by methoxide.

Introduction

Cerium oxide possesses outstanding catalytic properties in part due to its ability to rapidly change oxidation state between Ce^{3+} and Ce^{4+}. For this reason, cerium oxide is an excellent material to store and release oxygen, which is apparent in its phase diagram as a function of the chemical environment.[1] The oxygen storage capacity of cerium oxide is exploited in many of its applications. For instance, one of the primary function of cerium oxide in automotive catalytic converters that reduce the emission of harmful gases is the buffering of the oxygen content in the exhaust composition.[2,3] Applications for solid oxide fuel cells are based on the high oxygen conductivity in cerium oxide, which can be increased through doping and oxygen vacancy formation.[4] Although cerium oxide is catalytically active on its own, it also greatly enhances the activity of platinum group metals when used as support material[2] for industrially important reactions such as the water-gas-shift reaction or steam reforming of hydrocarbons. Decreasing cerium oxide particle size to the nanoscale[5] can have a significant impact on its catalytic properties[6] and has led to recent applications as an antioxidant adsorbing reactive species in cell cultures[7] and in vivo.[8] In nanoshaped materials, the exposure of certain facets is maximized, which may lead to a higher degree of control over catalytic performance. In addition, the use of faceted nanoparticles as catalyst material[9–11] facilitates fundamental understanding since results can be compared to surface science experiments using CeO_2 single crystal faces.[12,13]

The investigation of the structure-function relationship in catalysis over ceria has been the focus of our experimental work, where we utilize probe reactions to characterize acid/base properties, reducibility, and adsorption site geometries of the ceria catalyst. In particular, reactivity and selectivity in methanol decomposition has been measured as a function of surface structure and catalyst morphology in temperatur-programmed reactor experiments.[11] In these and in single crystal temperature programmed desorption (TPD) experiments[12,14,15] it was shown that activity and selectivity are controlled by the structure and the degree of reduction of the surfaces. While in previous UHV-based TPD experiments using oriented

cerium oxide surfaces[12,14,15] methyl formate was not observed, in reactor experiments using cerium oxide catalysts methyl formate was detected as a product in methanol oxidation reactions[16,17] and as a reaction intermediate in $Au - CeO_2$ nanorods.[18,19] It was reported[20] that in catalytic methyl formate formation over ReO_x/CeO_2 formate could act as the key intermediate. Conditions are certainly quite different between UHV and reactor experiments. While desorbed products or unreacted methanol do not return to the surface in UHV based TPD experiments, in the catalytic reactor, reactants are continuously supplied and products readsorb as the reaction proceeds and surface changes occur. In this work, we explore the formation of methyl formate using density functional theory (DFT) for different surface conditions (pristine and reduced) and adsorption sites.

The computational investigation of ceria and the catalytic conversion over ceria has now become a widely studied field. Work up to 2012 is summarized in a comprehensive review.[21] Some attention has to be paid to the fact that standard DFT methods are unable to describe the local character of the Ce 4f electrons in reduced ceria. However, the DFT+U method is commonly used to rectify the localization problem while introducing other issues,[21] such as the overstabilization of the reduced state.[22] Specifically, methanol adsorption and dissociation on ceria,[23–25] initial transformation,[26,27] formaldehyde oxidation,[30] specific aspects of methanol conversion on ceria,[31] and decomposition over vanadia/ceria[32] have been computationally studied. In-depth computational analysis of methanol conversion over ceria has been undertaken as well.[33,34] Methanol adsorbs on ceria at low temperature forming methoxide as a stable surface species through O-H cleavage. At higher temperatures methoxide undergoes stepwise dehydrogenation leading to formaldehyde and to the fully oxidized carbon oxide products. In most of the previous studies, isolated molecules have been considered although the importance of coadsorption has been shown.[22,31] In fact, neither the desorption of water at low temperature nor methanol at high temperature that were observed in TPD experiments of methanol on the fully oxidized ceria (111) surface can be explained without the interaction of adsorbates on the surface.[35] Of course, for the formation of methyl formate

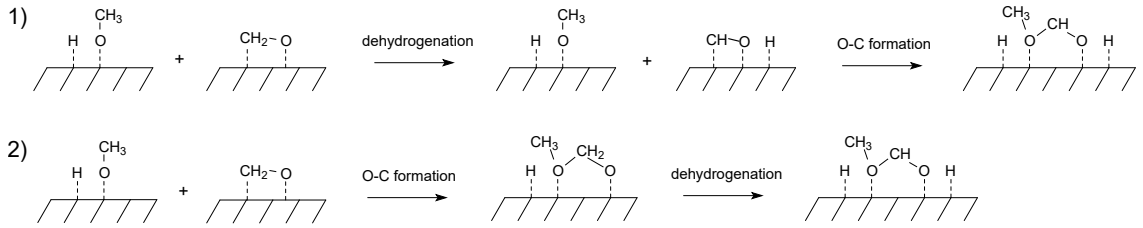

Figure 1: Reaction pathways to form methyl formate over ceria considered in this work.

during methanol conversion, surface species have to be available at conditions where reaction can occur, which lends one possible explanation for why methyl formate has not been seen in TPD experiments.[12,14,15] Surface species may desorb before reaction conditions are reached leading to a coverage that is too low for a significant number of bimolecular reactions to occur.

In the following, we examine the energetic requirements for methyl formate formation during methanol conversion over the most stable ceria (111) surface using the DFT+U method. Surface intermediates that are present during methanol decomposition and that serve as possible reactants are dissociatively adsorbed methanol (methoxide and hydroxide), chemisorbed formaldehyde (dioxymethylene[36]), and dehydrogenation products (formate) species. Starting from methanol and formaldehyde adsorbed on the surface, we investigate two possible pathways 1) dehydrogenation of chemisorbed formaldehyde followed by carbon-oxygen coupling 2) carbon-oxygen coupling of methoxide followed by dehydrogenation, both shown in 1. Note that dehydrogenation implies surface reduction, while carbon-oxygen coupling does not.

We assume that the reactants formaldehyde and methanol adsorb on the catalyst surface from the gas phase, where methanol forms methoxide and hydroxide without a significant barrier.[35] This is valid when modeling reactor experiments (as we do here), where product readsorption occurs. It prevents the saturation of surface oxygen sites with hydroxide that are produced during prior methoxide dehydrogenation. Although hydroxide on the surface due to methoxide dehydrogenation have been omitted during formaldehyde oxidation,[33] this is strictly not correct when comparing to TPD results since formaldehyde readsorption does

not occur and diffusion events would have to be considered. Note, it is necessary to maintain hydroxide from O-H cleavage in methanol during the simulations to model the correct ionic character of the surface species.[22] Because of previous surface reactions at the adsorption site; i.e., water formation and desorption,[35] adsorption may occur over an oxygen vacancy. In earlier work,[37,38] it was established that although the subsurface oxygen vacancy is more stable, due to the low barrier for oxygen migration, vacancies are readily available on the ceria surface through equilibration. It was also found[37,39] that at a moderate degree of reduction, vacancies are unlikely to cluster on the ceria surface and that a single vacancy is a good model for the partially reduced surface. Therefore, we consider three different surface configurations: the fully oxidized surface, the reduced surface where formaldehyde adsorbs over a single surface oxygen vacancy, and the reduced surface where methoxide occupies a single surface oxygen vacancy. Our results are presented below, following the description of the computational details.

Computational Details

All electronic structure calculations are carried out using the projector-augmented wave (PAW) method[40,41] as implemented in the Vienna ab initio simulation package (VASP).[42–45] We employ the PBE+U[46,47] functional to correct for shortcomings of standard DFT functionals due to the self-interaction error. A value of 5.0 eV for U is optimized to position occupied Ce 4f states about 1.3 eV above the oxygen 2p states in bulk Ce_2O_3.[48] Accordingly, a value of 4.5 eV has been used in recent methanol dehydrogenation studies mentioned above.[27,33,34] However, a lower value of U (2.0-3.0 eV) was recommended to better describe the redox chemistry over ceria surfaces[49] and in bulk.[50] A low U value was also suggested for the calculation of activation barriers.[51] In our work on methanol conversion over ceria,[22] we have found for reduction processes that a value of 3.0 eV agrees better with hybrid functional results[27] than a value of 5.0 eV because of an increasing overstabilization of the reduced state

with larger U. Performance variations of the DFT+U method depending on the chemical process have been observed previously.[28,29] Although it was reported that a minimum value of 3.0 eV is necessary for the f-electrons to localize on cerium,[52] we have found that a value of 3.0 eV is not always sufficient, particularly during geometry optimization. Since the correct defect geometry requires electron localization, we employ a value of 5.0 eV during geometry optimizations and reaction path determinations but execute single point calculations with a value of 3.0 eV for more accurate energy differences for redox processes. Transition states are confirmed by frequency analysis using a value of 5.0 eV for U. This strategy has been used in previous work by us on methanol conversion over ceria.[26,35] Unless otherwise noted, all energy values and reaction profiles reported throughout the paper are obtained at U = 3.0 eV while optimization paths in figures (including the Supporting Information) are given for U = 5.0 eV.

The (111) surface is constructed by stacking 9 atomic layers that are terminated by an oxygen layer and that extend periodically in the x- and y-directions. A vacuum layer of 15 Å is added in the z-direction to avoid interaction between slabs. We use a p(2x2) expansion of the surface cell that contains one dissociatively adsorbed methanol molecule and one dioxymethylene molecule for a carbon species coverage of 3.8 nm^{-2} simulating a fairly high coverage. The coverage in a reactor experiment is expected to be variable and to depend upon reactor conditions. However, high coverage is certainly a reasonable starting point in a UHV type TPD experiment.[12] The partially reduced surfaces are modelled by including a single oxygen vacancy in the top layer of the surface cell, which amounts to a vacancy coverage of 1.9 nm^{-2}. Removing one surface oxygen results in a vacancy with two electrons remaining in the surface. These electrons localize in cerium 4f-bands reducing two Ce^{4+} to Ce^{3+} ions that are nearest and next-nearest neighbors to the vacancy on the (111) surface.[37,38] We use the corresponding surface structure as a starting structure for adsorbate relaxation. However, we do not constrain the magnetic moments and the Ce^{3+} location may change during the relaxation.

During optimizations of minimum adsorbate structures and reaction paths, the top 6 atomic layers are relaxed while the remaining layers are fixed. We employ spin-polarized functionals, an energy cut off of 700 eV, a Γ-centered 3-3-1 Monkhorst-Pack k-point mesh, and dipole corrections perpendicular to the surface. Dispersion corrections are included through the D3 method by Grimme.[53] Minimum energy paths are optimized with the climbing image nudged elastic band method[54] (CI-NEB), where we use tools provided by the Henkelman group to set up the input. A positive adsorption energy indicates exothermic adsorption. The dissociative adsorption energy is defined as the sum of adsorption energy and dissociation energy. For the case of methanol, it is the difference between the energy of methoxide, coadsorbed hydroxide, and further adsorbates on the surface and the sum of energies of methanol and the surface with remaining adsorbates.

Results and Discussion

In reactor experiments of methanol conversion over ceria, methanol and formaldehyde are present in the gas phase and may adsorb on different parts of the catalyst that may or may not have undergone previous reduction. Here, we examine the fully oxidized ceria (111) surface and the partially reduced surface represented by a surface with an oxygen vacancy. Since either methanol or formaldehyde can adsorb over a vacancy, the following section is divided into three subsections according to the surface configuration considered (fully oxidized, dioxymethylene in vacancy, methoxide in vacancy) and given in 2. Note that methanol adsorbs dissociatively forming methoxide and hydroxide and formaldehyde adsorbs by interacting with a surface oxgygen forming dioxymethylene. Similarly, formyl (obtained through dehydrogenation of dioxymethylene) interacts with the surface producing formate. In all figures, species that are connected through bonds are rendered using covalent radii[56] including oxygen atoms that are part of the surface. We assume that for a coupling reaction to occur on the surface, the adsorbates have to be in neighboring positions. For

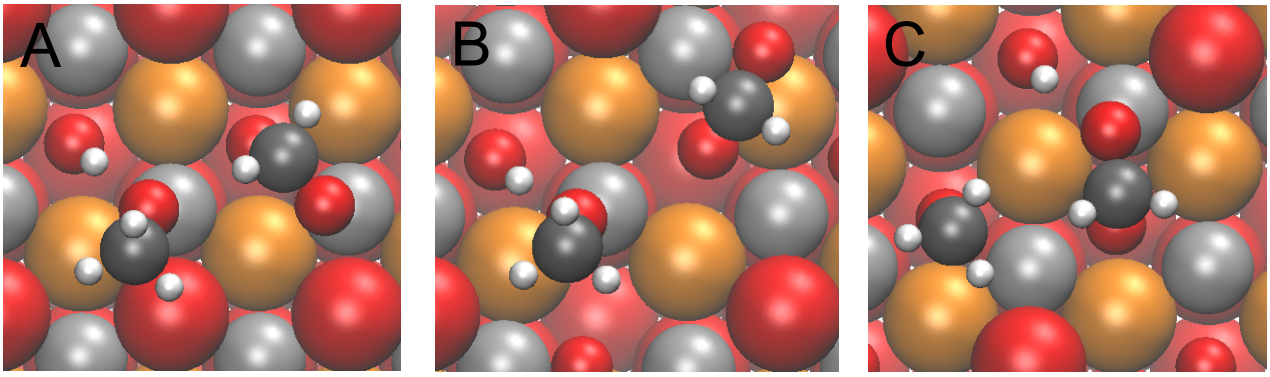

Figure 2: Ceria (111) surface configurations considered in this work; dioxymethylene and methanol dissociatively adsorbed on the A - fully oxidized surface, B - partially reduced surface with dioxymethylene in vacancy, C - partially reduced surface with methoxide in vacancy; top views, surface atoms are rendered using crystal ionic radii,[55] atoms forming covalent bonds are rendered using covalent radii,[56] red - general oxygen, orange - third layer oxygen, silver - cerium, gray - carbon, white - hydrogen.

each configuration shown in 2, we explore the pathways given in 1.

Oxidized Surface

The first step of pathway 1, 1 is the dehydrogenation of dioxymethylene starting from configuration A in 2. Hydrogen transfer may occur from dioxymethylene to a surface oxygen. Note, that there are only four oxygen atoms in the top layer of the surface cell of a p(2x2) expansion, one of them is bound to hydrogen, another to formaldehyde forming dioxymethylene. Of the two available surface oxygen atoms, one is too far from the hydrogen (4.6 Å) to be considered, the other is somewhat crowded by the neighboring methoxide. We calculate a barrier for hydrogen transfer to the latter oxygen of 1.71 eV using a U value of 3.0 eV (CI-NEB path is included in the Supporting Information, S1). Since dehydrogenation involves the reduction of cerium, the barrier strongly depends on the choice of the U parameter (see computational section). Our barrier calculated with U=5.0 eV is 1.27 eV. In the literature, an activation energy for dioxymethylene dehydrogenation without neighboring adsorbates of 1.53 eV[33] was reported using a value of 4.5 eV for U. The literature value for dehydrogenation of isolated dioxymethylene for U=4.5 eV lies between our values for U=3.0 eV and U=5.0

eV; albeit, one might expect the barrier for U=4.5 eV to be closer to the value for U=5.0 eV. However, this suggests that the crowding of the surface oxygen atom by neighboring methoxide does not cause an overestimation of the activation energy.

Another possible path for dioxymethylene dehydrogenation is through a formaldehyde intermediate that is not chemically bound to the surface. The formaldehyde intermediate forms from dioxymethylene without barrier (CI-NEB path is included in the Supporting Information, S2) and could rotate towards the surface to bring the hydrogen to be transferred closer to the surface than is possible in dioxymethylene. A second intermediate, formyl, could then be formed through dehydrogentation of weakly bound formaldehyde. The formyl intermediate can rotate to the surface yielding formate without barrier (CI-NEB path is included in the Supporting Information, S3). However, we were not able to find a transition state for hydrogen transfer from the weakly bound formaldehyde intermediate to the surface. Thermodynamic analysis shows that this path requires at least 1.50 eV activation energy.

Alternatively, we have identified a path with a significantly smaller activation barrier. Along this path, hydrogen is transferred from dioxymethylene to methoxide forming methanol (not identified as intermediate). This methanol then rotates and deposits hydrogen onto a surface oxygen without further activation barrier. The CI-NEB path (U=5.0 eV) together with selected structures along the path are shown in 3. The activation barrier for this path is with 0.59 eV (U=3.0 eV) considerably lower than unassisted hydrogen transfer from dioxymethylene to the surface (1.71 eV). Formate formation is exothermic with -1.36 eV (U=3.0 eV).

Similarly, the disproportionation of two methoxide to form methanol and dioxymethylene on the ceria (111) surface involves hydrogen transfer from the methyl group to oxygen of a second methoxide. Methoxide also promotes C-H cleavage in methoxide but to a lesser extent than in dioxymethylene. The activation energy for unassisted hydrogen transfer from methoxide to the ceria surface is 1.06 eV, while the barrier is reduced to 0.79 eV when hydrogen transfer is assisted by methoxide (1/2 monolayer caoverage).[35] Note that the barrier for

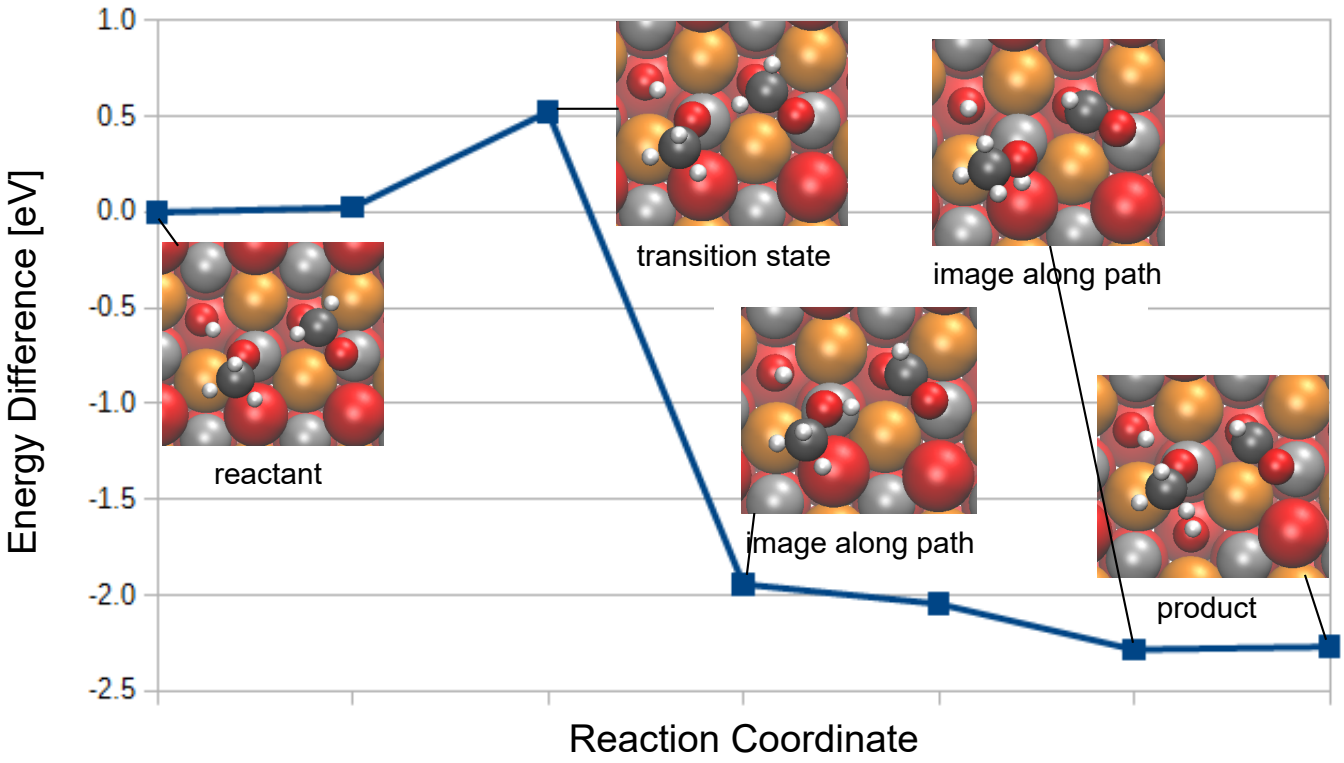

Figure 3: CI-NEB path (U=5.0 eV) for hydrogen transfer from dioxymethylene to surface oxygen via methanol formation on the fully oxidized ceria (111) surface; top views, rendering as in 2.

methoxide assisted dioxymethylene dehydrogenation is lower than the adsorption energy of methanol (in the reactant configuration considered here), which is 0.71 eV. This underlines the importance of adsorbate interactions on the surface. If methanol and formaldehyde adsorb adjacent to each other, dehydrogenation of dioxymethylene may occur before methanol desorption. High enough coverage of methoxide and dioxymethylene may be achieved in reactor experiments were formaldehyde and methanol are co-fed.

The second step of pathway 1, 1 is the oxygen-carbon bond formation between methoxide and formate (CI-NEB path is included in the Supporting Information, S4). This step has an activation barrier of 0.57 eV leading to methyl formate with an overall reaction energy of -0.92 eV. The reaction profile for methyl formate formation through pathway 1, 1 is given in 4.

In pathway 2, 1, the oxygen-carbon bond forms first between methoxide and dioxymethy-

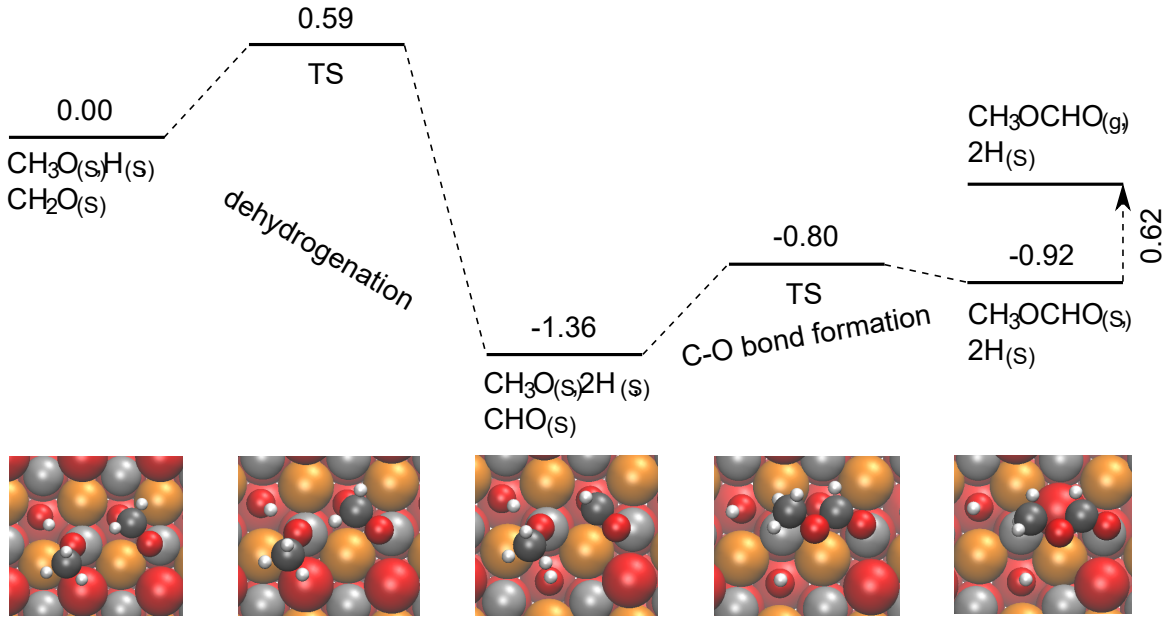

Figure 4: Reaction profile for methyl formate formation via pathway 1, 1 on the fully oxidized ceria (111) surface; energies in eV; (s) denotes species adsorbed on the surface, (g) denotes species in the gas phase; top views, rendering as in 2.

lene, which requires an energy of 0.62 eV (CI-NEB path is included in the Supporting Information, S5). Bond formation is thermoneutral. The subsequent dehydrogenation of the intermediate has an activation barrier of 0.96 eV leading to methyl formate (CI-NEB path is included in the Supporting Information, S6). The final product has a slightly different surface configuration than in pathway 1, 1 since the hydrogen is transferred from the intermediate to a different surface oxygen. 5 shows the reaction profile for methyl formate formation through pathway 2, 1.

When methanol is converted over ceria in a TPD experiment,[14] formaldehyde is formed above 500 K, which is sufficient to overcome a reaction barrier of above 1.0 eV for methoxide dehydrogentaon.[35] Since the reactant formaldehyde has to be present for methyl formate to be produced, the reactor temperature at which methyl formate is potentially formed is above 500 K. Assuming entropic factors of similar magnitude for dehydrogenation of the different species adsorbed on the ceria surface, we expect that at similarly high temperature than during methoxide dehydrogentaion pathway 1 and 2 for methyl formate formation are

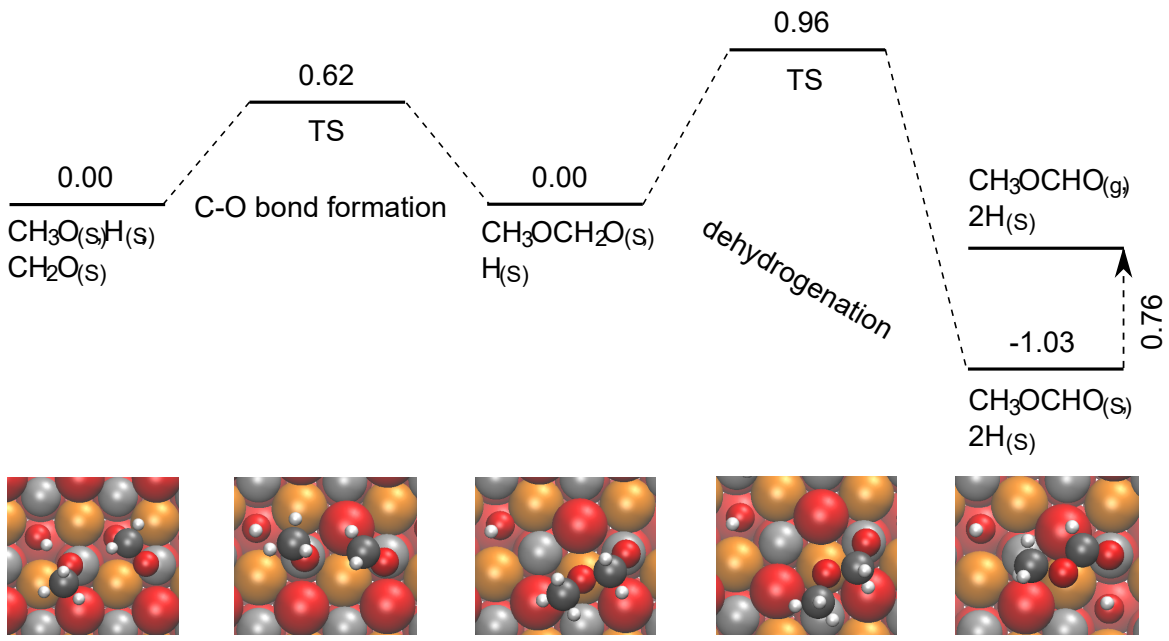

Figure 5: Reaction profile for methyl formate formation via pathway 2, 1 on the fully oxidized ceria (111) surface; energies in eV; (s) denotes species adsorbed on the surface, (g) denotes species in the gas phase; top views, rendering as in 2.

both attainable. The reaction barriers in pathway 1 are below 0.6 eV, which should lead to a significant amount of methyl formate being produced through pathway 1. However, in the reactant configuration 2 A, the dissociative adsorption energy of methanol is 0.71 eV and that of formaldehyde is 0.89 eV. The adsorption of both reactants next to each other is difficult to achieve. Certainly, in TPD experiments above 500 K configuration A in 2 is unlikely, while, in a reactor, the probability of that configuration to occur is a function of the partial pressure of methanol and formaldehyde. Removing the coadsorbed hydroxide through reaction or diffusion eliminates the recombination and desorption pathway. Adsorption over an oxygen vacancy also results in larger adsorption energies. The partially reduced surface is discussed in the following.

Reduced Surface, Dioxymethylene in Vacancy

In this section, we investigate methyl formate formation from methanol dissociatively adsorbed atop a cerium atom and formaldehyde adsorbed over an oxygen vacancy as shown in

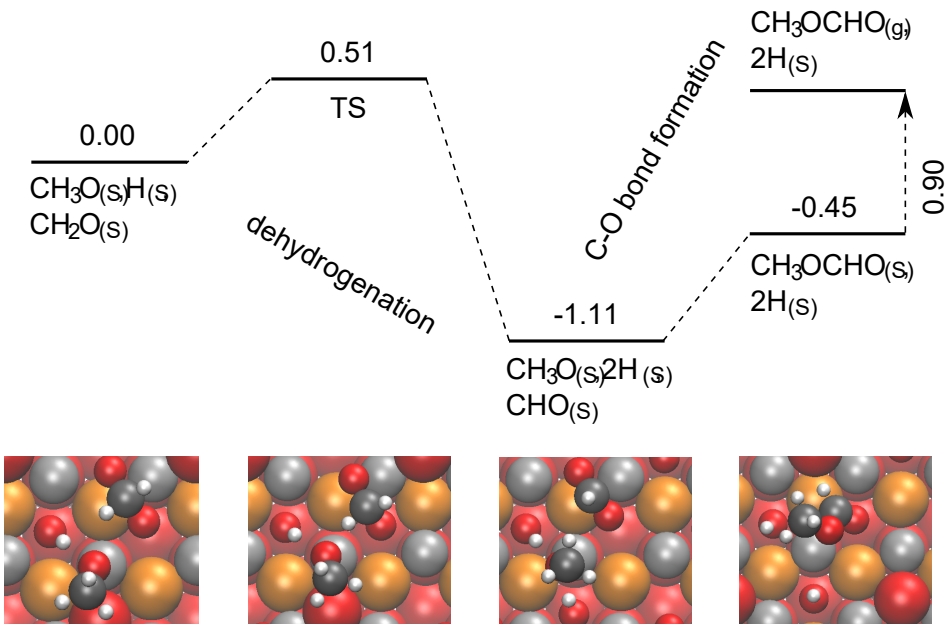

Figure 6: Reaction profile for methyl formate formation via pathway 1, 1 on partially reduced ceria (111) surface, dioxymethylene in vacancy; energies in eV; (s) denotes species adsorbed on the surface, (g) denotes species in the gas phase; top views, rendering as in 2.

2 B.

We first discuss methyl formate formation through pathway 1, 1. When formaldehyde adsorbs over an oxygen vacancy, it forms dioxymethylene as we have seen on the fully oxidized surface. However, in contrast to the oxidized surface, we are not able to isolate a formaldehyde intermediate that is not surface bound and we, therefore, do not study the corresponding path for dioxymethylene dehydrogenation through a formaldehyde intermediate. We consider dehydrogenation of dioxymethylene via hydrogen transfer to a surface oxygen and to methoxide. While configuration B in 2 is the starting configuration for pathway 2, it is not optimal for pathway 1. Dehydrogenation would result in formate that is unfavourably rotated for further coupling to methoxide. In addition, the hydrogen atoms in dioxymethylene are too far from methoxide oxygen for transfer. Instead, we use an energetically slightly higher starting configuration (by 0.25 eV) for pathway 1, where dioxymethylene is rotated by about 60° towards methoxide, see 6. Hydrogen transfer from dioxymethylene to the only available surface oxygen requires an activation energy of 1.60 eV (CI-NEB path is

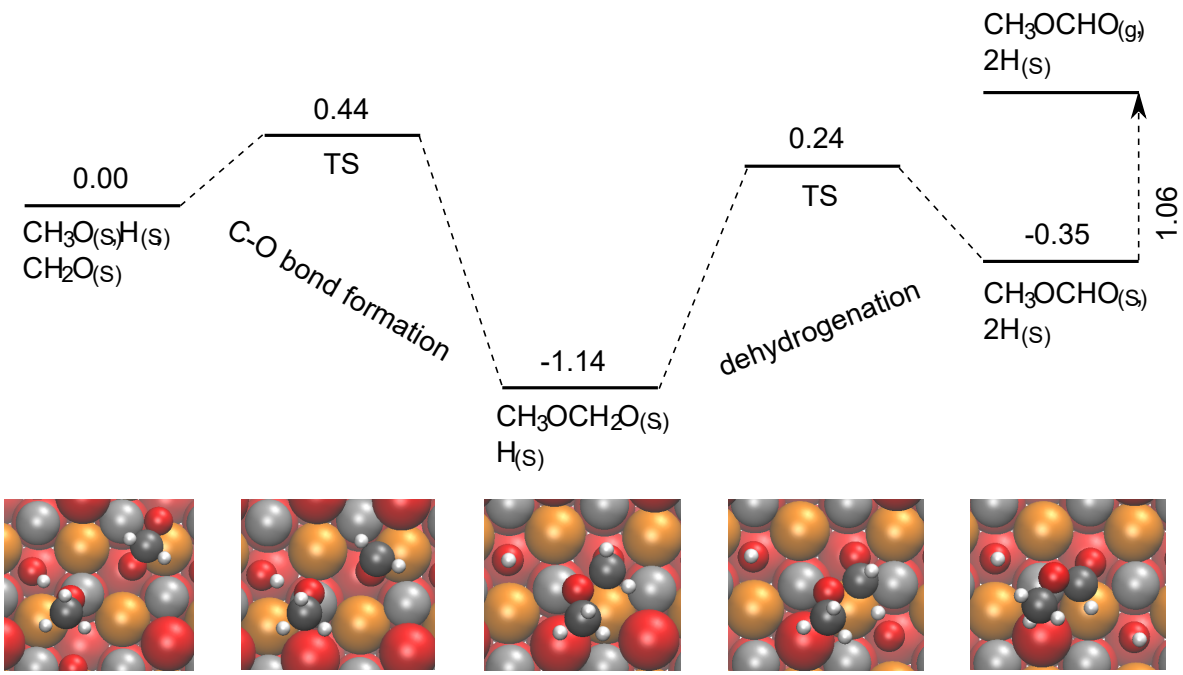

Figure 7: Reaction profile for methyl formate formation via pathway 2, 1 on partially reduced ceria (111) surface, dioxymethylene in vacancy; energies in eV; (s) denotes species adsorbed on the surface, (g) denotes species in the gas phase; top views, rendering as in 2.

included in the Supporting Information, S7). As on the oxidized surface, hydrogen transfer to methoxide has a much lower activation barrier of 0.51 eV. This time, we isolate methanol as an intermediate for hydrogen transfer from dioxymethylene to the surface (CI-NEB paths to yield methanol and for subsequent oxygen-hydrogen bond cleavage are included in the Supporting Information, S8 and S9, respectively). Formate formation is exothermic with a reaction energy of -1.11 eV. Coupling of methoxide and formate yielding methyl formate is endothermic but proceeds without barrier (CI-NEB path is included in the Supporting Information, S10). Pathway 1 is summarized in 6.

During our attempts to locate a formaldehyde intermediate that is not bound to a surface oxygen, optimization led to oxygen-carbon coupling between methoxide and dioxymethylene resulting in the intermediate of pathway 2, 1. However, the CI-NEB path for intermediate formation (included in the Supporting Information, S11) shows a plateau region that corresponds to formaldehyde that is not bound to a surface oxygen. This region is 0.44 eV higher in energy than the reactant configuration. Intermediate formation is with -1.14 eV

exothermic. The final hydrogen transfer step from intermediate to surface oxygen has an activation barrier of 1.38 eV (CI-NEB path is included in the Supporting Information, S12). 7 shows the reaction profile for methyl formate formation through pathway 2.

Comparing activation barriers on the fully oxidized surface and on the partially reduced ceria surface, where dioxymethylene is located in an oxygen vacancy, we observe an increase of the highest barrier in each path. However, in pathway 1, the maximum barrier is still only 0.66 eV for oxygen-carbon bond formation. Above 500 K, where reactant (formaldehyde) formation is observed,[14] the expected bottleneck for methyl formate formation to occur on the oxidized surface is the adsorption of both reactants next to each other on the surface, as discussed above. For configuration B in 2, the reaction barriers for methyl formate production through pathway 1 are still below the activation energy for methoxide dehydrogenation (above 1 eV[35]) to form formaldehyde but the adsorption energy of formaldehyde has increased from 0.89 eV on the oxidized surface to approximately 1.10 eV (estimated as the adsorption energy of formaldehyde over a vacancy next to methanol since the optimization of methoxide next to a vacancy leads to the migration of methoxide into the vacancy). This increases the probability for the occurrence of configuration B in a reactor experiment, where methanol is present in the gas phase and may adsorb next to a more stable dioxymethylene on the surface allowing methyl formate to form.

Reduced Surface, Methoxide in Vacancy

The last starting configuration for methyl formate formation we want to consider is configuration C in 2, where methoxide is located in an oxygen vacancy. However, a thermodynamic analysis reveals that the minimum activation barrier for oxygen-carbon bond formation along pathway 1, 1 is 2.73 eV and for pathway 2 is 1.95 eV. This can be deduced from the energy diagram in 8. The large energy requirements are due to the increase of the dissociative adsorption energy of methanol over an oxygen vacancy (by 1.47 eV) compared to the dissociative adsorption energy on the fully oxidized surface. In configuration B, 2, one dioxymethylene

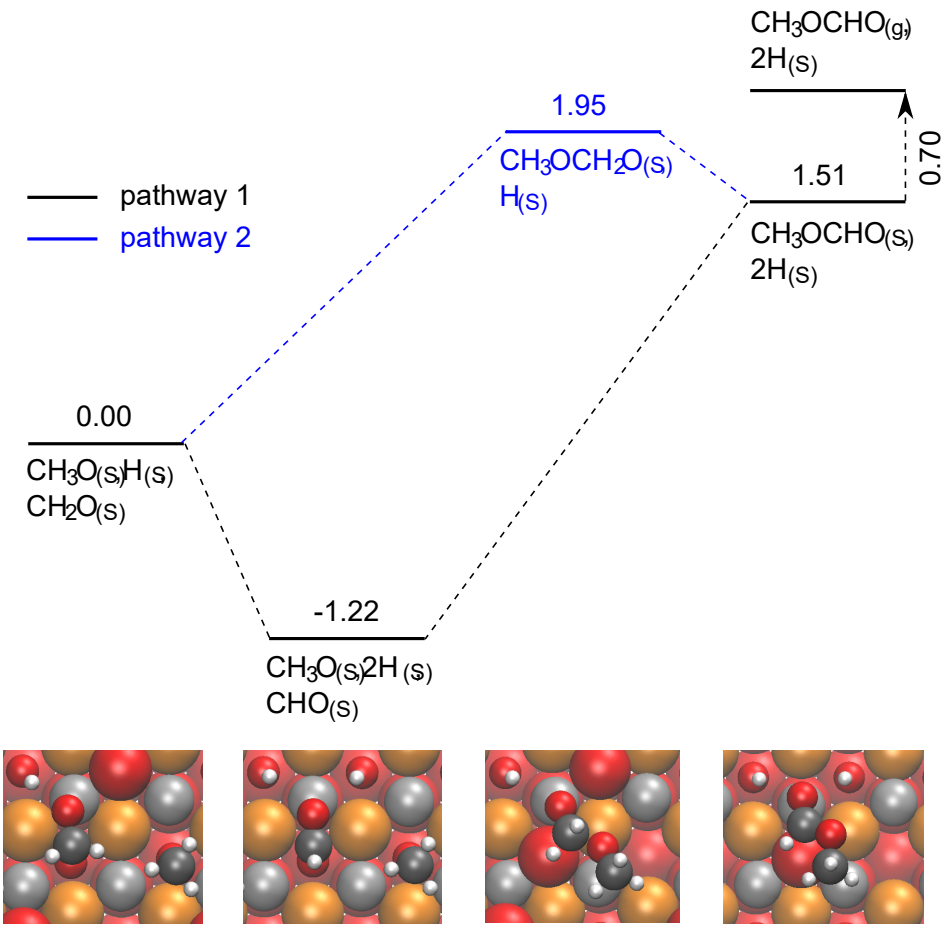

Figure 8: Energy diagram for methyl formate formation via pathway 1 and 2, 1 on partially reduced ceria (111) surface, methoxide in vacancy; energies in eV; (s) denotes species adsorbed on the surface, (g) denotes species in the gas phase; top views, rendering as in 2.

oxygen remains anchored to the oxygen vacancy as methyl formate is formed (6 and 7), while in configuration C, the methoxide must drift off the vacancy to form the oxygen-carbon bond in methyl formate (8). An unfilled surface oxygen vacancy is created that is associated with a large energy penalty.

Still, configuration C, 2 may contribute to overall methyl formate production. Methoxide can be replaced by another suitable adsorbate that is located next to the vacancy. If, for instance, hydroxide is situated next to the methoxide filled vacancy, hydroxide can push methoxide to an atop position. In the reactant configuration hydroxide/methoxide exchange requires an energy of 0.63 eV. In the formate configuration along pathway 1 this replacement requires 0.43 eV (CI-NEB paths are included in the Supporting Information, S13 and S14,

respectively). Activation energies for methyl formate formation are then expected to be similar to what we have shown for configuration A, 2 on the fully oxidized surface.

Another possible route for methoxide adsorbed in an oxygen vacancy to participate in methyl formate production is through dehydrogenation. The activation barrier for C-H cleavage of an isolated methoxide in a vacancy is 1.28 eV.[26] The resulting dioxymethylene in the vacancy could then react with coadsorbed methoxide following the reaction paths outlined in above section "Reduced Surface, Dioxymethylene in Vacancy".

Finally, we discuss potential generalizations of the work presented herein. Previously, it was shown that the barrier for dehydrogentation of methoxide is similar for the (111), (100), and (110) surfaces but that the adsorption energies of surfaces species vary significantly for different crystallographic orientations.[26,33,34] It is reasonable to deduce that dehydrogentation of dioxymethylene is similarly promoted by methoxide on all ceria surfaces resulting in lowered barriers for methyl formate formation. However, differences in residence time of surface species change the probability for finding formaldehyde and methanol adsorbed adjacent to each other. We, therefore, predict that methyl formate production is increased on the (100) surface due to larger adsorption energies of methanol and formaldehyde on the surface. We also believe that the promotion of dioxymethylene dehydration by methoxide is not restricted to the ceria surface but should be observable on other oxide surfaces as well. Badlani and Wachs[17] have shown that activity in redox active oxides, those oxides that yield methyl formate and formaldehyde as primary products in methanol oxidation, is highly correlated with methoxide decomposition temperature. Their remarkable correlation supports the conclusion that methoxide C-H bond cleavage is the rate limiting step, but does not provide insight into the pathways for coupling that leads to methyl formate or the selectivity between formaldehyde vs methyl formate. The present results provide initial insight into how formaldehyde/dioxymethylene adsorption energy and its methoxide promoted dehydrogenation may combine to control this selectivity in the entire group of redox active oxides.

Conclusion

Using DFT, we studied methyl formate formation during methanol conversion on the (111) ceria surface. We excluded the possibility of direct coupling between two methoxide and considered two pathways of methyl formate production starting from methanol dissociatively and formaldehyde adsorbed on the surface, the latter forming dioxymethylene. In pathway 1, dehydrogenation of dioxymethylene occurs prior to oxygen-carbon bond formation, while in pathway 2, the oxygen-carbon bond is formed first followed by dehydrogenation of the intermediate. Previously, we calculated activation barriers for methoxide dehydrogenation of about 1 eV and above.[22,35] Correspondingly, formaldehyde production was observed above 500 K in experiment.[14] On the fully oxidized surface pathways 1 and 2 have a maximum barrier below 1 eV. The maximum barrier of pathway 1 is only 0.59 eV. However, the adsorption energies of methanol and formaldehyde are below 0.9 eV and both species desorb at temperatures above 500 K that allow for prior methoxide dehdrogenation (reactant formation). In reactor experiments, readsorption occurs but the probability of both reactants adsorbing adjacent to each other is low. This probability can be increased by prolonging the residence time of either adsorbate. The desorption pathway of methanol can be eliminated by hydroxide removal through water formation.[35] Another option is the increase of the adsorption energy by adsorbate placement in an oxygen vacancy. When dioxymethylene is located in a vacancy, pathway 1 continues to have a lower maximum barrier than pathway 2 with 0.66 eV for pathway 1. The large increase of the dissociative adsorption energy for methanol at a vacancy resulted in activation barriers for oxygen-carbon bond formation of above 2 eV for either pathway. Still, reduction of the ceria surface is anticipated to enhance methyl formate formation through stabilization of either formaldehyde or methanol since methoxide trapped in a vacancy can easily be exchanged with a suitable coadsorbates (i.e. hydroxidel) or proceed to dehydrogenation forming formaldehyde that is active for methyl formate production.

Importantly, we found that methoxide promotes dehydrogenation of dioxymethylene ei-

ther on the oxidized surface or in an oxygen vacancy. The activation barrier for C-H cleavage of about 1 eV and above,[22,35] which we also observed here for C-H cleavage in the intermediate of pathway 2, is lowered to below 0.6 eV. We predict that if methanol and formaldehyde are co-fed in a reactor experiment, a significant amount of methyl formate is produced at low temperature.

Acknowledgements

This research was sponsored by the Laboratory Directed Research and Development Program of Oak Ridge National Laboratory, managed by UT-Battelle, LLC, for the U.S. Department of Energy. This research used resources of the National Energy Research Scientific Computing Center, a Department of Energy Office of Science User Facility supported by the Office of Science of the U.S. Department of Energy under Contract No. DE-AC02-05CH11231.

Supporting Information Available: Supporting information contains CI-NEB (U=5eV) paths on the oxidized ceria (111) surface: for hydrogen transfer from dioxymethylene to surface oxygen, for formaldehyde intermediate formation from dioxymethylene, for formate formation from formyl intermediate, for oxygen-carbon bond formation between methoxide and formate, for oxygen-carbon bond formation between methoxide and dioxymethylene, for intermediate dehydrogenation; CI-NEB (U=5eV) paths on the partially reduced ceria (111) surface: for hydrogen transfer from dioxymethylene in oxygen vacancy to surface oxygen, for hydrogen transfer from dioxymethylene in oxygen vacancy to methoxide oxygen, for oxygen-hydrogen bond cleavage in methanol, for oxygen-carbon bond formation between methoxide and formate in oxygen vacancy, for oxygen-carbon bond formation between methoxide and dioxymethylene in oxygen vacancy, for intermediate dehydrogenation in oxygen vacancy, for methoxide/hydroxide exchange in oxygen vacancy in reactant configuration, for methoxide/hydroxide exchange in oxygen vacancy in formate configuration.

This material is available free of charge via the Internet at http://pubs.acs.org.

References

(1) Zinkevich, M.; Djurovic, D.; Aldinger, F. Thermodynamic Modelling of the Cerium-Oxygen System. *Solid State Ionics* **2006**, *177*, 989 – 1001.

(2) Gorte, R. J. Ceria in Catalysis: From Automotive Applications to the Water Gas Shift Reaction. *AICHE* **2010**, *56*, 1126 – 1135.

(3) Chen, H.-Y.; Chang, H.-L. Development of Low Temperature Three-Way Catalysts for Future Fuel Efficient Vehicles. *Johnson Matthey Technol. Rev.* **2015**, *59*, 64 – 67.

(4) Trovarelli, A., Fornasiero, P., Eds. *Catalysis by Ceria and Related Materials*, 2nd ed.; Catalytic Science Series; Imperial College Press: London, 2013; Vol. 12.

(5) Yuan, Q.; Duan, H. H.; Li, L. L.; Sun, L. D.; Zhang, Y. W.; Yan, C. H. Controlled Synthesis and Assembly of Ceria-Based Nanomaterials. *J. Colloid Interface Sci.* **2009**, *335*, 151 – 167.

(6) Melchionna, M.; Fornasiero, P. The Role of Ceria-Based Nanostructured Materials in Energy Applications. *Materials Today* **2014**, *17*, 349 – 357.

(7) Lee, S. S.; Song, W.; Cho, M.; Puppala, H. L.; Nguyen, P.; Zhu, H.; Segatori, L.; Colvin, V. L. Antioxidant Properties of Cerium Oxide Nanocrystals as a Function of Nanocrystal Diameter and Surface Coating. *ACS Nano* **2013**, *7*, 9693 – 9703.

(8) Yokel, R. A.; Tseng, M. T.; Dan, M.; Unrine, J. M.; Graham, U. M.; Wu, P.; Grulke, E. A. Biodistribution and Biopersistence of Ceria Engineered Nanomaterials: Size Dependence. *Nanomed-Nanotechnol* **2013**, *9*, 398 – 407.

(9) Li, M.; Wu, Z.; Overbury, S. H. Surface Structure Dependence of Selective Oxidation of Ethanol on Faceted CeO_2 Nanocrystals. *J. Cat.* **2013**, *306*, 164 – 176.

(10) Mann, A. K. P.; Wu, Z. L.; Overbury, S. H. In *Catalysis by Materials with Well-Defined Structures*; Wu, Z., Overbury, S. H., Eds.; Elsevier, 2015; The Characterization and Structure-Dependent Catalysis of Ceria with Well-Defined Facets, pp 71 – 97.

(11) Wu, Z. L.; Li, M. J.; Mullins, D. R.; Overbury, S. H. Probing the Surface Sites of CeO_2 Nanocrystals with Well-Defined Surface Planes via Methanol Adsorption and Desorption. *ACS Catalysis* **2012**, *2*, 2224 – 2234.

(12) Mullins, D. R.; Albrecht, P. M.; Calaza, F. C. Variations in Reactivity on Different Crystallographic Orientations of Cerium Oxide. *Top. Catal.* **2013**, *56*, 1345 – 1362.

(13) Mullins, D. The Surface Chemistry of Cerium Oxide. *Surf. Sci. Rep.* **2015**, *70*, 42 – 85.

(14) Mullins, D. R.; Robbins, M. D.; Zhou, J. Adsorption and Reaction of Methanol on Thin-Film Cerium Oxide. *Surface Science* **2006**, *600*, 1547 –1558.

(15) Albrecht, P. M.; Mullins, D. R. Adsorption and Reaction of Methanol over $CeO_x(100)$ Thin Films. *Langmuir* **2013**, *29*, 4559 – 4567.

(16) Tatibouet, J. M. Methanol Oxidation as a Catalytic Surface Probe. *Appl. Catal. A: General* **1997**, *148*, 213 – 252.

(17) Badlani, M.; Wachs, I. E. Methanol: A "Smart" Chemical Probe Molecule. *Catalysis Letters* **2001**, *75*, 137 – 149.

(18) Yi, N.; Si, R.; Saltsburg, H.; Flytzani-Stephanopoulos, M. Steam Reforming of Methanol over Ceria and Gold-Ceria Nanoshapes. *Applied Catalysis, B: Environmental* **2010**, *95*, 87 – 92.

(19) Boucher, M. B.; Yi, N.; Gittleson, F.; Zugic, B.; Saltsburg, H.; Flytzani-Stephanopoulos, M. Hydrogen Production from Methanol over Gold Supported on ZnO and CeO_2 Nanoshapes. *J. Phys. Chem. C* **2011**, *115*, 1261 – 1268.

(20) Liu, J.; Zhan, E.; Cai, W.; Li, J.; Shen, W. Methanol Selective Oxidation to Methyl Formate over ReO_x/CeO_2 Catalysts. *Catalysis Letters* **2008**, *120*, 174 – 280.

(21) Paier, J.; Penschke, C.; Sauer, J. Oxygen Defects and Surface Chemistry of Ceria: Quantum Chemical Studies Compared to Experiment. *Chem. Rev.* **2013**, *113*, 3949 – 3985.

(22) Beste, A.; Overbury, S. H. Hydrogen and Methoxy Coadsorption in the Computation of the Catalytic Conversion of Methanol on the Ceria (111) Surface. *Surface Science* **2016**, *648*, 242 – 249.

(23) Beste, A.; Mullins, D. R.; Overbury, S. H.; Harrison, R. J. Adsorption and Dissociation of Methanol on the Fully Oxidized and Partially Reduced (111) Cerium Oxide Surface: Dependence on the Configuration of the Cerium 4f Electrons. *Surface Science* **2008**, *602*, 162 – 175.

(24) Mei, D.; Deskins, N. A.; Dupuis, M.; Ge, Q. Density Functional Theory Study of Methanol Decomposition on the CeO_2(110) Surface. *J. Phys. Chem. C* **2008**, *112*, 4257 – 4266.

(25) Yang, C.; Bebensee, F.; Nefedov, A.; Wöll, C.; Kropp, T.; Komissarov, L.; Penschke, C.; Moerer, R.; Paier, J.; Sauer, J. Methanol Adsorption on Monocrystalline Ceria Surfaces. *J. Catal.* **2016**, *336*, 116 – 125.

(26) Beste, A.; Overbury, S. H. Dehydrogenation of Methanol to Formaldehyde Catalyzed by Pristine and Defective Ceria Surfaces. *Phys. Chem. Chem. Phys.* **2016**, *18*, 9990 – 9998.

(27) Kropp, T.; Paier, J. Reactions of Methanol with Pristine and Defective Ceria (111) Surfaces: A Comparison of Density Functionals. *J. Phys. Chem. C* **2014**, *118*, 23690 – 23700.

(28) Capdevila-Cortada, M.; Łodziana, Z.; Løpez, N. Performance of DFT+U Approaches in the Study of Catalytic Materials. *ACS Catalysis* **2016**, *6*, 8370 – 8379.

(29) Bennett, L.-J.; Jones, G. The Influence of the Hubbard U Parameter in Simulating the Catalytic Behaviour of Cerium Oxide. *Phys. Chem. Chem. Phys.* **2014**, *16*, 21032 – 21038.

(30) Teng, B.-T.; Jiang, S.-Y.; Yang, Z.-X.; Luo, M.-F.; Lan, Y.-Z. A Density Functional Theory Study of Formaldehyde Adsorption and Oxidation on CeO_2 (111) Surface. *Surface Science* **2010**, *604*, 68 – 78.

(31) Lustemberg, P. G.; Bosco, M. V.; Bonivardi, A.; Busnengo, H. F.; Ganduglia-Pirovano, M. V. Insights into the Nature of Formate Species in the Decomposition and Reaction of Methanol over Cerium Oxide Surfaces: A Combined Infrared Spectroscopy and Density Functional Theory Study. *J. Phys. Chem. C* **2015**, *119*, 21452 – 21464.

(32) Kropp, T.; Paier, J.; Sauer, J. Support Effect in Oxide Catalysis: Methanol Oxidation on Vanadia/Ceria. *J. Am. Chem. Soc.* **2014**, *136*, 14616 – 14625.

(33) Capdevila-Cortada, M.; García-Melchor, M.; López, N. Unraveling the Structure Sensitivity in Methanol Conversion on CeO_2: A DFT + U Study. *J. Cat.* **2015**, *327*, 58 – 64.

(34) Kropp, T.; Paier, J. Activity versus Selectivity of the Methanol Oxidation at Ceria Surfaces: A Comparative First-Principles Study. *J. Phys. Chem. C* **2015**, *119*, 23021 – 23031.

(35) Sutton, J. E.; Overbury, S. H.; Beste, A. Coadsorbed Species Explain the Mechanism of Methanol Temperature-Programmed Desorption on CeO_2(111). *J. Phys. Chem. C* **2016**, *120*, 7241 – 7247.

(36) Zhou, J.; Mullins, D. R. Adsorption and Reaction of Formaldehyde on Thin-Film Cerium Oxide. *Surf. Sci.* **2006**, *600*, 1540 – 1546.

(37) Sutton, J. E.; Beste, A.; Overbury, S. H. Origins and Implications of the Ordering of Oxygen Vacancies and Localized Electrons on Partially Reduced CeO_2(111). *Phys. Rev. B* **2015**, *92*, 144105.

(38) Ganduglia-Pirovano, M. V.; Da Silva, J. L. F.; Sauer, J. Density-Functional Calculations of the Structure of Near-Surface Oxygen Vacancies and Electron Localization on CeO_2(111). *Phys. Rev. Lett.* **2009**, *102*, 026101.

(39) Murgida, G. E.; Ganduglia-Pirovano, M. V. Evidence for Subsurface Ordering of Oxygen Vacancies on the Reduced CeO_2(111) Surface Using Density-Functional and Statistical Calculations. *Phys. Rev. Lett.* **2013**, *110*, 246101.

(40) Blochl, P. E. Projector Augmented-Wave Method. *Phys. Rev. B* **1994**, *50*, 17953 – 17979.

(41) Kresse, G.; Joubert, D. From Utrasoft Pseudopotentials to the Projector Augmented-Wave Method. *Phys. Rev. B* **1999**, *59*, 1758 – 1775.

(42) Kresse, G.; Hafner, J. Ab Initio Molecular Dynamics for Liquid Metals. *Phys. Rev. B* **1993**, *47*, 558 – 561.

(43) Kresse, G.; Hafner, J. Ab Initio Molecular Dynamics Simulation of the Liquid-Metal-Amorphous-Semiconductor Transition in Germanium. *Phys. Rev. B* **1994**, *49*, 14251 – 14269.

(44) Kresse, G.; Furthmüller, J. Efficiency of Ab Initio Total Energy Calculations for Metals and Semiconductors Using a Plane-Wave Basis Set. *Comput. Mat. Sci.* **1996**, *6*, 15 – 50.

(45) Kresse, G.; Furthmüller, J. Efficient Iterative Schemes for Ab Initio Total Energy Calculations Using a Plane-Wave Basis Set. *Phys. Rev. B* **1996**, *54*, 11169 – 11186.

(46) Perdew, J. P.; Burke, K.; Ernzerhof, M. Generalized Gradient Approximation Made Simple. *Phys. Rev. Lett.* **1996**, *77*, 3865 – 3868.

(47) Dudarev, S. L.; Botton, G. A.; Savrasov, S. Y.; Humphreys, C. J.; Sutton, A. P. Electron-Energy-Loss Spectra and the Structural Stability of Nickel Oxide: An LSDA+U Study. *Phys. Rev. B* **1998**, *57*, 1505 – 1509.

(48) Watkins, M. B.; Foster, A. S.; Shluger, A. L. Hydrogen Cycle on CeO_2 (111) Surfaces: Density Functional Theory Calculations. *J. Phys. Chem. C* **2007**, *111*, 15337 – 15341.

(49) Huang, M.; Fabris, S. CO Adsorption and Oxidation on Ceria Surfaces from DFT+U Calculations. *J. Phys. Chem. C* **2008**, *112*, 8643 – 8648.

(50) Loschen, C.; Carrasco, J.; Neyman, K. M.; Illas, F. First-Principles LDA+U and GGA+U Study of Cerium Oxides: Dependence on the Effective U Parameter. *Phys. Rev. B* **2007**, *75*, 035115–1 – 8.

(51) Calaza, F. C.; Xu, Y.; Mullins, D. R.; Overbury, S. H. Oxygen Vacancy-Assisted Coupling and Enolization of Acetaldehyde on CeO_2(111). *J. Am. Chem. Soc.* **2012**, *134*, 18034 – 18045.

(52) Castleton, C. W. M.; Kullgren, J.; Hermansson, K. Tuning LDA+U for Electron Localization and Structure at Oxygen Vacancies in Ceria. *J. Chem. Phys.* **2007**, *127*, 244704–1 – 11.

(53) Grimme, S.; Antony, J.; Ehrlich, S.; Krieg, H. A Consistent and Accurate Ab Initio Parametrization of Density Functional Dispersion Correction (DFT-D) for the 94 Elements H-Pu. *J. Chem. Phys.* **2010**, *132*, 154104–1 – 154104–19.

(54) Henkelman, G.; Uberuaga, B. P.; Jónsson, H. A Climbing Image Nudged Elastic Band Method for Finding Saddle Points and Minimum Energy Paths. *J. Chem. Phys.* **2000**, *113*, 9901 – 9904.

(55) Shannon, R. D. Revised Effective Ionic Radii and Systematic Studies of Interatomic Distances in Halides and Chalcogenides. *Acta Cryst* **1976**, *A32*, 751 767.

(56) Cordero, B.; Gómez, V.; Platero-Prats, A. E.; Revés, M.; Echeverría, J.; Cremades, E.; Barragán, F.; Alvarez, S. Covalent Radii Revisited. *Dalton Trans.* **2008**, *21*, 2832 2838.

TOC Graphic

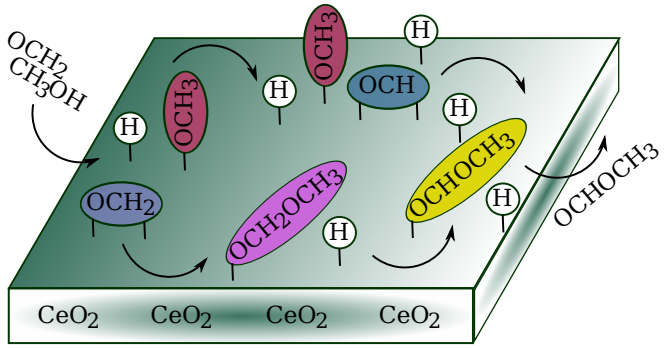
OCH2
CH3OH
H
OCH3
H
OCH3
H
OCH
H
OCH2
OCH2OCH3
H
OCHOCH3
H
OCHOCH3
CeO2
CeO2
CeO2
CeO2